

DETECTION OF CRACK INITIATION FOR FRACTURE TOUGHNESS EVALUATION OF THERMOSET AND THERMOPLASTIC FIBRE- REINFORCED MATERIALS

Markus G. R. Sause¹, Michael Greisel² and Nora Schorer¹

¹Institute of Materials Resource Management, University of Augsburg, D-86135 Augsburg, Germany
Email: markus.sause@mrm.uni-augsburg.de, Web Page: <http://www.mrm.uni-augsburg/en/groups/sause/>

²Institute of Physics, University of Augsburg, D-86135 Augsburg, Germany

Keywords: Fracture mechanics, digital image correlation, acoustic emission

Abstract

In order to compare the performance of data reduction procedures recommended in ASTM D 5528 and ASTM D 7905, we conducted fracture mechanics tests in four different material systems combined with acoustic emission measurements and digital image correlation analysis. The four different carbon fibre reinforced materials were selected to span the range from brittle matrix materials (epoxy, PEEK) to ductile matrix materials (PPS, PA6). In all cases evaluated, the force values obtained from the acoustic emission onset defined by the Historic index proved as most relevant values for the calculation of mode I and mode II fracture toughness values.

1. Introduction

In order to measure the initiation fracture toughness of fibre-reinforced materials, several test standards are available. For mode I, mode II or mixed-mode fracture toughness, established ASTM, ISO and EN standards evaluate the onset of crack initiation based on significant changes in the load displacement curves or based on observations by in-situ optical microscopy. However, the definition of an effective crack length in the sense of the flaw size required for fracture mechanics is compromised by plastic deformation before crack initiation, or by polymer crazing and by microscopic crack branching before macroscopic crack growth [1–3]. The occurrence of these phenomena cannot be properly distinguished by the classical data reduction procedures of the established standards. In this study, we combine fracture mechanics tests with digital image correlation and acoustic emission to aid in the assessment of crack initiation loads as considered relevant for the calculation of the fracture toughness values. Both methods have proven as effective tools to monitor the first onset of microscopic damage [4, 5] and have been proposed previously to this extent. To determine the first damage onset via acoustic emission, trend monitoring techniques, such as the Historic Index as defined in ASTM E2478-11 have already been proposed as reliable tools [6]. We also reported previously on the use of digital image correlation for this purpose [4].

The aim of the present study is the comparison of four fibre-reinforced composites, being vastly different in their failure behaviour. All samples are subject to the same data reduction routines and may act as principle test cases to demonstrate the broad range of applicability.

2. Experimental

2.1. Specimen preparation

Within this study, we investigated four representative types of fibre-reinforced materials. We choose a carbon fibre epoxy prepreg material (Sigrafil CE 1250-230-39), and carbon fibre reinforced tapes made from polyphenylene sulfide (FORTRON 1140L4 Torayca T700S), polyether ether ketone

(Tenax-E TPUD PEEK HTS45) and polyamide 6 (Celstran CFR-TP PA6 CF60-01). The according nomenclature follows the scheme fibre/matrix, e.g. C50/E20, T700/PPS, HTS45/PEEK and C/PA6. This selection represents a broad range of material grades, spanning from almost brittle failure to highly ductile failure. All materials were fabricated as unidirectional layups in accordance with the material supplier's recommendations, using thin ($< 30 \mu\text{m}$) foils to act as pre-crack. All specimens were cut to nominal dimensions of 250 mm x 20 mm (length x width) and nominal thickness of 3 mm, except for C/PA6 with 3.7 mm thickness.

2.2. Acquisition settings

To analyse the crack initiation, we conducted mode I fracture toughness tests following the general recommendations of ASTM D 5528 and mode II fracture toughness test following ASTM D 7905. All materials are tested in standard climate conditions (23°C, 50% RH) after material specific conditioning cycles.

In addition to the recording of force displacement curves, we used multi-resonant acoustic emission sensors (type WD) to monitor for the occurrence of microscopic crack growth as potential precursors to the macroscopic crack initiation for both test configurations. The principle acquisition settings are based on 40 dB_{AE} preamplification, 35 dB_{AE} threshold level, 10 MSP/s sampling rate, a bandpass from 20 kHz to 1 MHz and trigger settings adapted to the specific test mode and material sound velocity. For mode I tests, we used two acoustic emission sensors (type WD and HD2WD) attached to the double cantilever beam specimen, allowing a linear Δt -based source localization. Using this information, continuous R-curves were obtained by as well [7], but are not further discussed herein, as the focus is on the detection of the first onset of damage. For mode II tests, we used one acoustic emission sensors (type WD) attached to the load nose and/or attached to the specimen. In addition, we applied high-resolution 3D digital image correlation (system ARAMIS 12M) to visualize the interlaminar crack growth as strain concentrations in the full-field strain measurement. In each test configuration, five or more specimens were tested to obtain the reported mean fracture toughness values and their margin of error.

2.3. Data reduction procedure

Besides the standardized data reduction routine of ASTM D 5528 and ASTM D 7905 to evaluate the interlaminar crack initiation, we added an evaluation approach using acoustic emission and one approach using digital image correlation.

For acoustic emission, the key challenge stems from the proper evaluation of the recorded signals. As most conservative approach, the first acoustic emission signal acquired during the load could be used to define the onset. Because of the sensitivity of the method, this approach is error-prone to detection of outliers which are fracture events on the microscopic scale, but do not necessarily indicate the growth of the macroscopic delamination. Accordingly, proposals were made for averaging of the first acoustic emission signals, which are still biased in the number of signals to use. To overcome these challenges, the use of progressive trend analysis methods has emerged. While some of them are properly functional for huge signal numbers only (e.g. exponentially weighted moving average in [8]), the Historic index has emerged as appropriate tool to quantify the first onset of damage. Figure 1-a and 1-b demonstrate the different acoustic emission based concepts in application to one test sample. The occurrence of the first acoustic emission signal may constitute the most conservative indicator to assess the occurrence of first damage. However, because of its sensitivity to outliers (i.e. generation of acoustic emission in insert region, at load blocks, ...) this is typically not very stable. Instead, averaging of the first N signals is used more often, so this reduces the effect of outliers. The number N of signals used for the averaging does add some bias to the evaluation and needs to be selected carefully. Instead, because of its sharp rise, the Historic index appears as a more reliable tool to safely identify the true damage onset and is thus investigated more closely herein. For the present study, we have chosen to take the first onset of acoustic emission signals based on the average of the first ten signals.

For digital image correlation evaluation, figure 2 presents an example of the typical strain concentration due to the included pre-crack in a mode II test configuration before and after crack growth. The corresponding data reduction routine is the screening of the image series for the occurrence of such sudden advances, which allows to evaluate the corresponding propagation load with an accuracy corresponding the image acquisition rate.

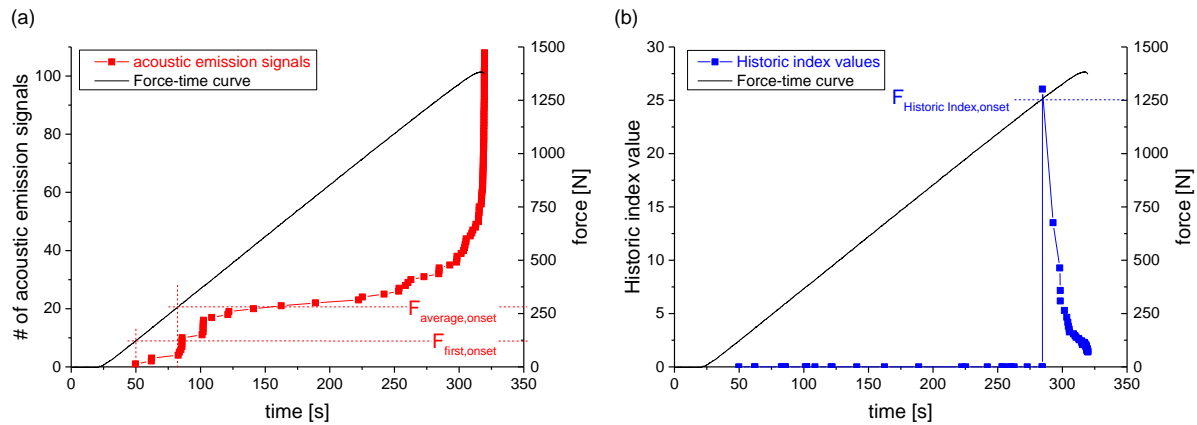


Figure 1. Example for evaluation of acoustic emission based onset criteria using first onset or average of first signals (a) and Historic index (b) to evaluate load at crack initiation in mode II test.

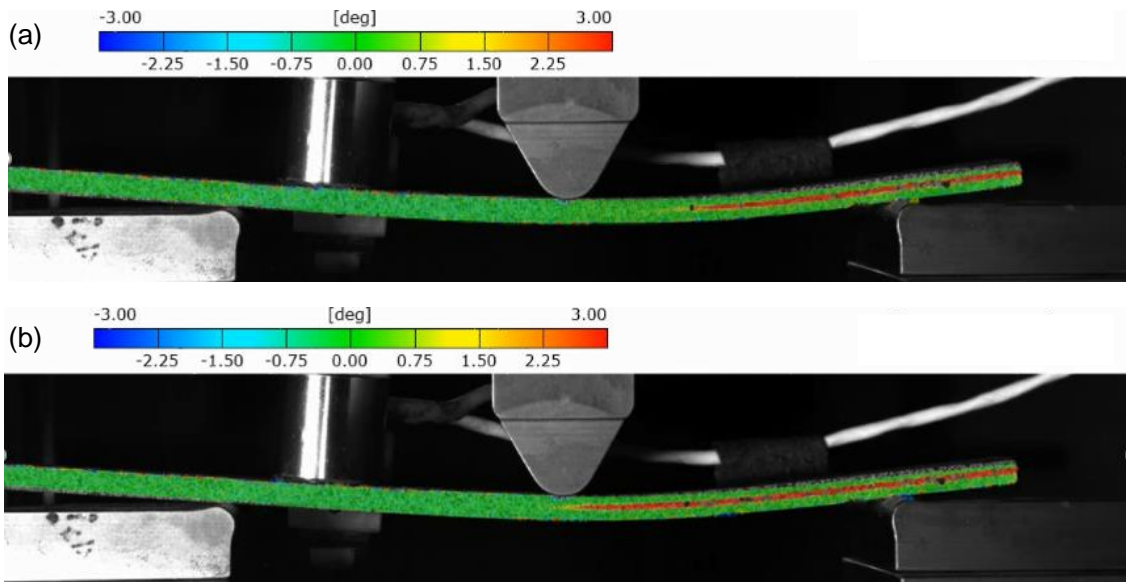


Figure 2. Example for strain concentration effect in shear angle measurement during mode II test before (a) and after (b) crack growth.

3. Results

In the following, we present the results of the two chosen test configurations for each of the four material types.

3.1. Mode I test (DCB)

All results of the tested materials are summarized in table 1. Following the procedure of ASTM D 5528, the three criteria NL, VIS and 5%MAX are evaluated from the load-displacement curves. The

corresponding evaluation of force values is shown in figure 3 for one representative example of each material. In addition, two more loads are evaluated based on the acoustic emission measurements, corresponding to first onset of acoustic emission signals (ONSET) and the onset based on the Historic index (HI). For all examples of figure 3, the Historic index is plotted superimposed to the load-time curve with vertical dashed lines to indicate the occurrence of each acoustic emission based criterion.

Table 1. Evaluated Mode I fracture toughness results.

Specimen Type	<i>ASTM D 5528-NL</i> [J/m ²]	<i>ASTM D 5528-VIS</i> [J/m ²]	<i>ASTM D 5528-5%MAX</i> [J/m ²]	<i>AE ONSET</i> [J/m ²]	<i>AE HI</i> [J/m ²]
C50/E201	318 ± 54	315 ± 79	356 ± 24	315 ± 29	365 ± 45
T700/PPS	222 ± 22	700 ± 93	968 ± 88	289 ± 80	716 ± 112
HTS45/PEEK	955 ± 149	1044 ± 140	1040 ± 145	930 ± 56	1001 ± 111
C/PA6	680 ± 58	1220 ± 98	1220 ± 98	732 ± 51	1182 ± 39

For the epoxy matrix system C50/E201 of figure 3-a, brittle failure was predominantly observed in mode I loading. Accordingly, the onset of non-linearity (NL) and the visible crack onset (VIS) coincide. Still, the load increases beyond that point and the force maximum is evaluated instead of the 95% slope, as the intersection is not reached prior to the maximum load value (5%MAX). Remarkably, the ONSET coincides with the NL and VIS range, while the HI falls in the same range as the 5%MAX criterion. The most likely reason for the early non-linearity is the occurrence of microscopic crack branching prior to macroscopic crack growth, while the latter is better represented by the 5%MAX or the HI criterion.

For the more ductile material T700/PPS shown in figure 3-b, a relatively low NL is evaluated, which is again credited for microscopic crack formation and the occurrence of plastic deformation. The early formation of cracks is supported by the occurrence of first acoustic emission and a very similar range for the NL and ONSET criterion. The first visible damage VIS is correlated to a small dip in the load-time curve and falls in the same range as the HI criterion, indicating the occurrence of the macroscopic crack growth. The evaluation of the 5%MAX criterion is based on the 95% slope in some of the specimens, in others based on the maximum force value. In all specimens, the 5%MAX load is significantly higher than the detected onset of macroscopic crack propagation, the increase of load beyond the macroscopic onset mostly attributed to crazing of the thermoplastic polymer and plastic deformation.

The failure mode of HTS45/PEEK as seen in figure 3-c was found to be relatively brittle. The occurrence of first non-linearity (NL) falls in the same range as the ONSET criterion. For PEEK, a certain degree of microscopic crack branching before macroscopic crack growth is expected as well. Other than for the previous cases, the visible onset VIS occurs at the maximum force 5%MAX, which is the same range as indicated by the HI criterion.

For the testing of C/PA6, first attempts were made using materials with accelerated conditioned according to DIN EN ISO 1110. For this condition, the typical failure mode observed was a kinking of the cantilever arm, as seen in figure 4, even at significantly increased laminate thickness. Accordingly, a second set of specimens was prepared using drying in vacuum conditions at 80°C process to decrease the humidity incorporated in the PA6 matrix. As seen in the example of figure 3-d, the testing was carried out successfully in this material state, as the overall failure mode was more brittle. Similar to the previous material systems, the evaluated NL range coincides well with the ONSET criterion, which allows to conclude, that this is the occurrence of first microcracking in the material. For all of

the specimens tested, the HI criterion also coincides with the range of the 5%MAX, which is an indication for the occurrence of significant damage as posed by the onset of the macroscopic crack growth.

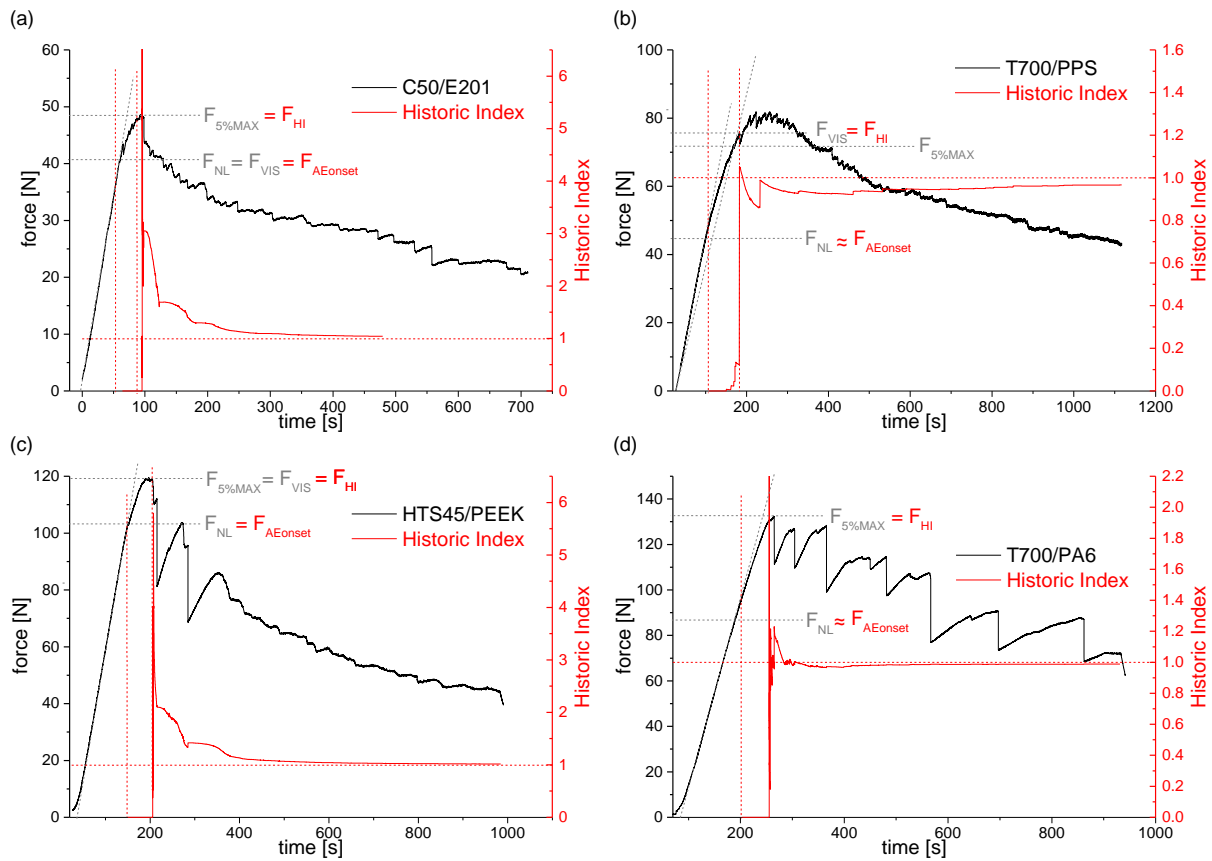


Figure 3. Example for force evaluation using ASTM D 5528 criteria and acoustic emission criteria for one example of each material (a-d).

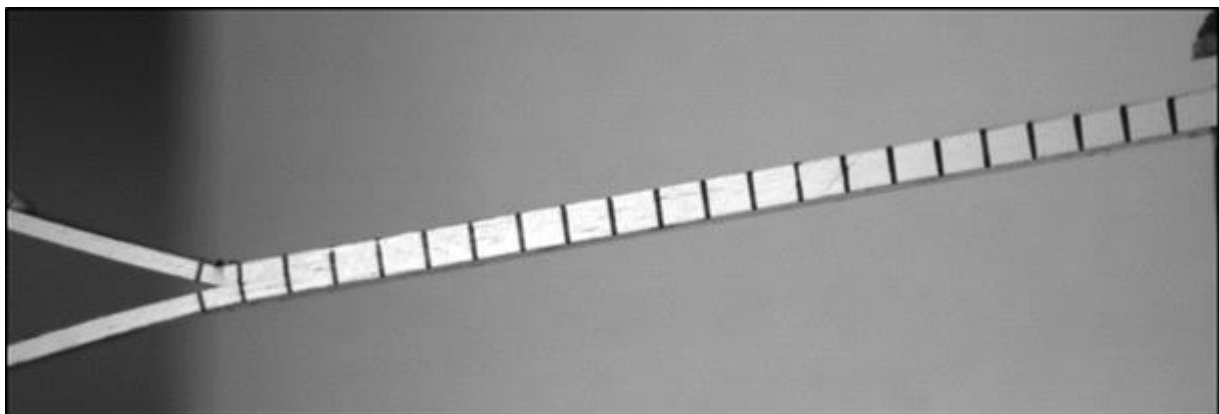


Figure 4. Typical failure mode for 3.7 mm C/PA6 (after accelerated conditioning), tested in DCB configuration under standard climate conditions (23°C, 50% RH).

3.2. Mode II test (ENF)

Following the procedure of ASTM D 7905, the pre-cracked fracture toughness results are summarized in table 2. In addition, the acoustic emission results are evaluated in the same way as for the DCB tests to obtain the ONSET and HI criterion. Moreover, the digital image correlation was used to evaluate

the validity of the test procedure, specifically for the ductile matrix polymers. In figure 5a-d representative examples for each material are shown.

Table 2. Evaluated Mode II fracture toughness results.

Specimen Type	ASTM D 7905 [J/m ²]	AE ONSET [J/m ²]	AE HI [J/m ²]
C50/E201	1198 ± 104	1121 ± 187	1198 ± 104
T700/PPS	3722 ± 1227	647 ± 234	1536 ± 207
HTS45/PEEK	1668 ± 115	1073 ± 73	1613 ± 103
C/PA6	-	-	-

For the C50/E201 material, the failure mode observed is quite brittle as seen in the curve of figure 5-a. Accordingly, the ASTM D 7905 standard recommends the use of the maximum load value to obtain the mode II fracture toughness. In all cases, the acoustic emission initiates prior to the force maximum, indicating the initiation of microscopic damage. In all specimens, the measured onset of the Historic index happens at the load maximum. Accordingly, HI yields identical values for the fracture toughness as the standard evaluation. This behaviour is in agreement with the observation of the corresponding DCB tests discussed in section 3.1.

The general material behaviour of the T700/PPS seen in figure 5-b was observed to be more ductile. For this case, the strict evaluation according to the standards (max. force) yields an extraordinary high fracture toughness value. Other than that, both acoustic emission based values (ONSET and HI) provide a conservative estimate of the fracture toughness values. The ONSET value estimates an early onset of less than a factor of five of the ASTM standard value, which might readily be too conservative as no according crack growth was observed in the accompanying DIC measurements at these load levels. Instead, the HI value appears to be most significant to detect the initiation of macroscopic crack growth, as the respective load value coincides with the visual observation of crack growth in the DIC measurements.

For the HTS45/PEEK specimens one representative example is shown in figure 5-c. In these specimens, the ONSET values precede the force maximum significantly. Not correlated to a significant trend change in the force-displacement curve, this early occurrence of acoustic emission is expected to originate from microcracking of the PEEK matrix. The HI values are evaluated at load levels slightly lower than the force maximum for some specimens and at the force maximum for other specimens. Within the margin of error, this results in identical values of the mode II fracture toughness as the ASTM standard.

For the C/PA6 material, a representative load-displacement curve is shown in figure 5-d. According to the ASTM D 7905 one might be tempted to evaluate the force maximum for the calculation of the mode II fracture toughness. However, in several configurations tested (i.e. variation of laminate thickness, dry PA6 state, conditioned PA6 state) no valid failure mode, i.e. macroscopic crack growth was reached. The typical failure modes are shown in figure 6. For the C/PA6 tested in dry state, the beam undergoes kinking at the position of the insert instead of crack growth (cf. figure 6-a). Attempts were made to reduce the distance between crack tip and load nose, which resulted in a shift of the failure location towards the position of the load nose as seen in figure 6-b. Accordingly, no macroscopic crack growth is reached either. In all cases, an early onset of acoustic emission is observed (ONSET). Based on the DIC observations, this does not indicate the occurrence of macroscopic crack growth, but is rather expected to occur from microscopic crack initiation at the

position of the crack tip, but also at the later position of failure (insert tip or load nose). For the Historic index, the evaluation consistently results in values lower than one for the duration of the experiment. This is a good indication that the criticality of the acoustic emission has not yet been reached and therefore acts as another independent proof of the absence of macroscopic crack initiation.

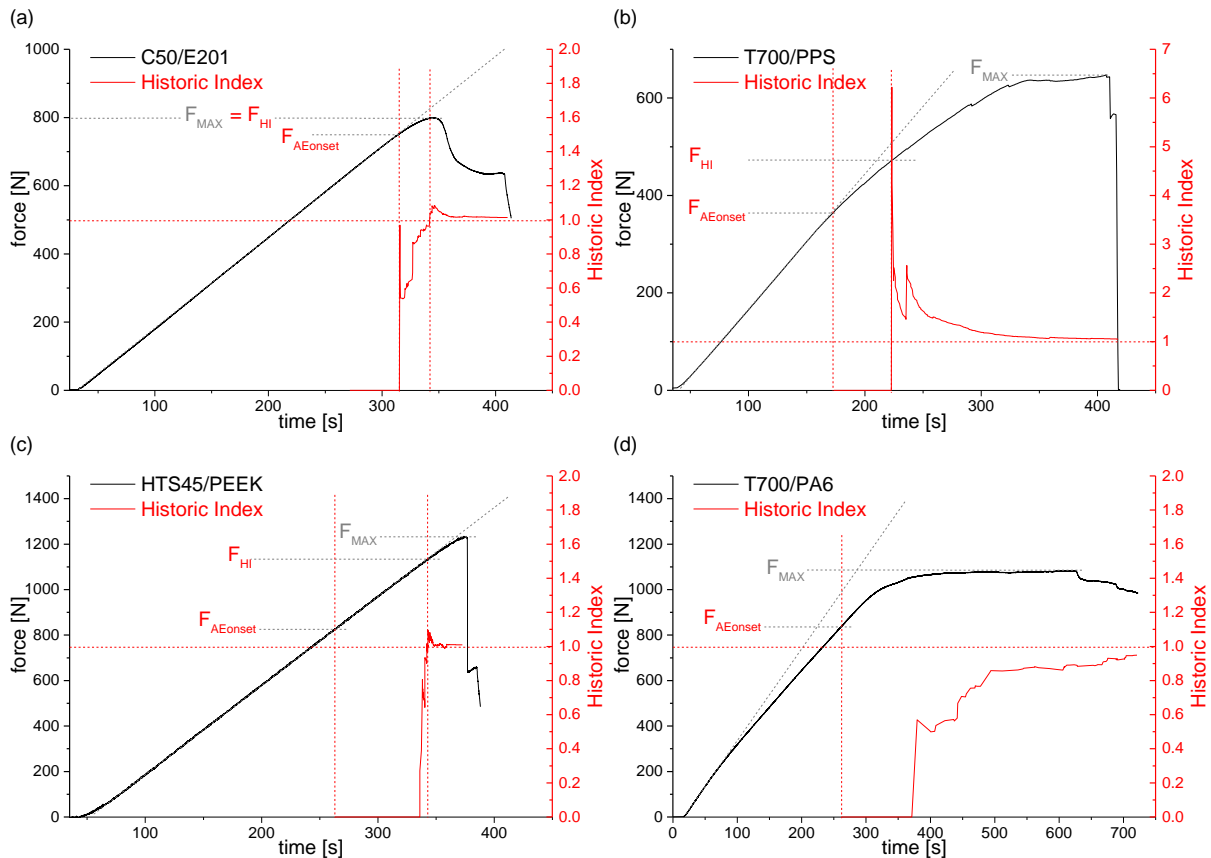


Figure 5. Example for force evaluation using ASTM D 7905 criteria and acoustic emission criteria for one example of each material (a-d).

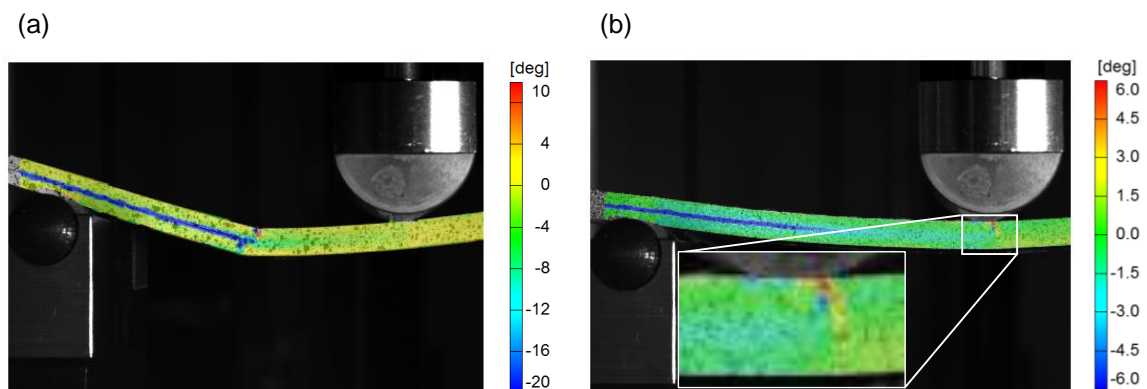


Figure 6. Typical failure mode in compression at crack tip (a) and in compression at load nose (b) for 3.7 mm C/PA6 (dry state), tested in ENF configuration under standard climate conditions (23°C, 50% RH).

4. Conclusions

Using four representative material systems, a comparison of evaluation criteria following ASTM D 5528 and ASTM D 7905 was made vs. onset loads obtained from acoustic emission measurements and comparison with digital image correlation results. Clear trends for the significance of each criterion

were detected. Depending on the material system, the onset of acoustic emission signals can be used to detect the first onset of microscopic damage, typically related to the start of a non-linear force-displacement relation. The macroscopic growth of damage, as relevant for fracture mechanics calculation was consistently identified better across all four materials by the Historic index. Depending on the material type, the HI result coincides with the VIS or 5%MAX criterion in mode I testing. For mode II, the typical estimate using the force maximum appears to be misleading for those cases with significant matrix ductility. While the C/PA6 case no macroscopic crack growth could be induced in the standard settings, for the remaining cases, the HI criterion successfully identified the onset of macroscopic crack growth. Instead, the first onset of acoustic emission appears to be more sensitive to the occurrence of microscopic crack initiation, which precedes the macroscopic failure. Beyond these two experimental configurations, the application of acoustic emission to test in mixed-mode loading or in application to hybrid laminates, sandwich materials or adhesives appears straightforward and is expected to increase the reliability of force onset values for crack initiation significantly.

Acknowledgments

We thank the BMBF for funding the projects MAIplast and MAIpolymer within the leading edge cluster MAI Carbon and the Free State of Bavaria for funding the project ComBo within the BayernFIT initiative. Moreover, we would like to thank Florian Henne (LCC TU Munich) and Dr.-Ing. Iman Taha (Fraunhofer IGCV) for fabrication of the test specimens.

References

- [1] Tijssens, M.G., van der Giessen, E., Sluys, L.J.: *Simulation of mode I crack growth in polymers by crazing*. Int. J. Solids Struct. **37**, 7307–7327 (2000).
- [2] Blackman, B.R.K., Brunner, A.J., Williams, J.G.: *Mode II fracture testing of composites: a new look at an old problem*. Eng. Fract. Mech. **73**, 2443–2455 (2006).
- [3] Brunner, A. J., Blackman, B. R. K., Davies P.: *A status report on delamination resistance testing of polymer-matrix composites*. Eng. Fract. Mech. 2779–2794 (2008).
- [4] Sause, M.G.R.: *In Situ Monitoring of Fiber-Reinforced Composites*. Springer International Publishing, Cham (2016).
- [5] Bohse, J., Chen, J.: *Acoustic Emission Examination of Mode I, Mode II and Mixed-Mode I/II Interlaminar Fracture of Unidirectional Fiber-Reinforced Polymers*. J. Acoust. Emiss. **19**, 1–10 (2001).
- [6] Baran, I.J., Nowak, M.B., Chłopek, J.P., Konsztowicz, K.J.: *Acoustic Emission from Microcrack Initiation in Polymer Matrix Composites in Short Beam Shear Test*. J. Nondestruct. Eval. **37**, 7 (2018).
- [7] Moosburger-Will, J., Sause, M.G.R., Horny, R., Horn, S., Scholler, J., Llopard Prieto, L.: *Joining of carbon fiber reinforced polymer laminates by a novel partial cross-linking process*. J. Appl. Polym. Sci. **132**, n/a-n/a (2015).
- [8] Abraham, A.R.A., Johnson, K.L., Nichols, C.T., Saulsberry, R.L., Waller, J.M.: *Use of Statistical Analysis of Acoustic Emission Data on Carbon-Epoxy COPV Materials-of-Construction for Enhanced Felicity Ratio Onset Determination - JSC-CN-26080*. (2011).